Available online at www.sciencedirect.com
SCIENCE DIRECT®
ELSEVIER
Nuclear Instruments and Methods in Physics Research B 236 (2005) 495–500
NIM B
Beam Interactions with Materials & Atoms
www.elsevier.com/locate/nimb

Magnetic polymeric microspheres for protein adsorption

M.C.F.C. Felinto [a], D.F. Parra [a], A.B. Lugão [a,*], M.P. Batista [a], O.Z. Higa [a], M. Yamaura [a], R.L. Camilo [a], M.T.C.P. Ribela [a], L.C. Sampaio [b]

[a] *Instituto de Pesquisas Energéticas e Nucleares, Av. Professor Lineu Prestes 2242, Cidade Universitária, São Paulo, SP.CEP: 05508-000, Brazil*
[b] *Centro Brasileiro de Pesquisas Físicas, Rio de Janeiro-RJ CEP 22290-180, Brazil*

Available online 1 June 2005

Abstract

Magnetic beads consisting of polymer-coated manganese ferrite nanoparticles were prepared by the precipitation reaction of manganese ferrite into the channels of methyl methacrylate polymer beads by sodium hydroxide, resulting in MnMagBead. MnMagBead was characterized by infrared spectra (FTIR), thermogravimetric analysis of TGA/DTG and indicates the presence of –CO (carbonyl) groups and the $MnFe_2O_4$ on the beads. Magnetization measurements were obtained at room temperature in magnetic fields up to 10 KOe using a vibrating sample magnetometer. Introductory Protein adsorption biological tests were processed using labeled I-125 albumin (BSA), and the activity was measured in a gamma counting spectrometer.

These superparamagnetic beads exhibit the capacity to bind biological molecules such as proteins like albumin, with a good capability (5×10^{-6}) μg/100 mg of beads as compared with other magnetic resins studied in our group.

1. Introduction

In recent years, the design and the synthesis of nanometer scale particles have been the focus of intense fundamental and applied research, with special emphasis on their size dependent properties [1–3]. Magnetic separation has been widely applied to various aspects in biotechnology and biomedical engineering, such as cell separation [4,5], immobilized enzyme [6], protein separation [7], target drugs [8] and antibody immobilization [9]. Magnetic separation is relatively rapid, and carriers with peculiar properties are necessary.

Magnetic resins are usually composed of two parts: a magnetic core, which is often made up of inorganic magnetic nanoparticles, such as Fe_3O_4, $MnFe_2O_4$, $CoFe_2O_4$, etc., and the polymeric shell recovering the magnetic core [10–20]. Moreover, considering their magnetic properties, separation is relatively rapid and easy, requiring a simple

* Corresponding author. Tel.: +55 11 3816 9334; fax: +55 11 3816 9325.
E-mail address: ablugao@ipen.br (A.B. Lugão).

0168-583X/$ - see front matter © 2005 Elsevier B.V. All rights reserved.
doi:10.1016/j.nimb.2005.04.056

Fig. 1. MnMagBead spheres.

apparatus, compared to centrifugal separation [19]. Many different techniques have been developed for preparation of magnetic particles [11,12,18–21]. The chemical and physical properties of magnetic materials containing metal particles depend on the size and distribution of the particles and the presence (or lack) of interactions among their surface, matrix and contaminants [13]. Therefore, this requires the need for controlling the size and distribution of the particles on the matrix material. In this respect, the use of aqueous suspension polymerization has not been evaluated for preparing iron/network material composites. The present work was aimed at magnetic and morphological characterization of network polyacrylate microspheres containing iron/manganese nanoparticles dispersed on their channels. It was also tested for the retention of bovine serum albumin, BSA, by these magnetic beads (Fig. 1).

2. Experimental procedures

2.1. Synthesis of microbeads

Magnetic particles were prepared by the chemical co-precipitation method [22–25]. The starting material was a solution of $FeCl_3 \cdot 6H_2O$ and $MnCl_2 \cdot 4H_2O$ with a molar relationship concentration 1:2, respectively. Amberlite XAD#7, nonionic polymeric adsorbent polyacrylate resin microbeads (grain size <297 μm and channel diameter <90 Å) from Rohm and Haas Co. (Lot No. 03001TG certificated by Aldrich) were procured from Aldrich and used after treatment with methanol and water to eliminate impurities and monomer species. These beads were put into iron/manganese chloride solution overnight to make them swell. After that the beads were reacted with NaOH (5 M) for precipitating the ferrite. To ensure magnetization of the nanoparticles after precipitation reaction, the material was heated for 1 h at 98 °C under constant stirring. The magnetic beads were cooled down to room temperature and then washed with deionized water until they reached pH ~7, in order to remove unreacted chemicals. Finally, the wet magnetic beads were dried and used for characterization and absorption experiments.

2.2. Characterization

Characterization of magnetic beads was carried out using infrared spectrometry, thermal analyses and magnetic measurements.

The infrared spectra of the samples were used to provide information about the nature of the interaction of the microbeads and the magnetic ferrite nanoparticles. These spectra were recorded in the range from 4000 to 400 cm^{-1} in KBr pellets by using a Bomem model MB102 FTIR spectrophotometer. Thermogravimetric (TG) curves were obtained with a SDTA-822 thermobalance (Mettler Toledo), using samples with approximately 7 mg in sapphire crucibles, under a dynamic nitrogen atmosphere (50 mL min^{-1}), at a heating rate of 10 °C min^{-1}. Magnetization measurements were performed at room temperature in magnetic fields up to 10 kOe using a vibrating sample magnetometer (Princeton Applied Research, model 530).

2.3. Methodology for protein absorption

Obtention of labeled I-125 albumin. In order to quantify the adsorption of protein, to the beads, the BSA was labeled with ^{125}I by the chloramine T method [26]. The labeled protein corresponds to 41.1% of total BSA. The labeled BSA was separated from the bulk protein using a Sephadex

chromatographic column and the specific activity was 37.15 μCi/μg.

Contactation of ^{125}I-BSA with the MnMagBeads. In order to perform equilibrium experiments, pre-equilibrated samples were kept in contacted with a buffer (pH = 7.35) composed of the following reagents: 0.2 g KCl, 80 g NaCl, 0.2 g KH_2PO_4 and 1.15 g Na_2HPO_4 per liter of water. The samples were previously weighed (100 mg) and conditioned with the buffer and kept in with the ^{125}I Albumin (37.15 μCi/μg). The experiments were done under static conditions and the batch method was used. The samples were further gently rinsed until the radioactivity of the surface remained constant. The samples were shaken for 10 and 60 min. The resin was easily separated by the solution using a magnet. The quantification was done using a gamma counter, Beckman Gamma 4000 (60% of efficiency).

3. Results and discussion

The process for obtention of ferrite nanoparticles, $MnFe_2O_4$, follows the reaction given below and was carried out in an aqueous medium:

$$Mn^{2+} + 2Fe^{3+} + 8OH^- \rightarrow MnFe_2O_4 + 4H_2O \qquad (I)$$

The size of particles was confined to a maximum of about 90 Å [27], which was the diameter size of the bead channel.

Fig. 2 shows the infrared spectra of these magnetic beads, MnMagBeads, manganese ferrite, the beads without magnetic particles and the MnMagBeads after thermal heating until 400 °C. It was possible to confirm that no interaction between the polymer matrix and the magnetic core occurs. The two broad bands at ~3439 and ~1640 cm^{-1} can be ascribed to the O–H stretching vibration and OH bending mode of the free OH group, respectively [28,29] and bands at ~580 cm^{-1} ascribed to νM_{Td}–O–M_{Oh} appear in all spectra except for Acrylate XAD#7. Attribution of the transition for these materials is given in Table 1.

TG data from MnMagBeads presented in Fig. 3 showed one first event in the range of 57–159.83 °C with a mass loss of 8.3% corresponding

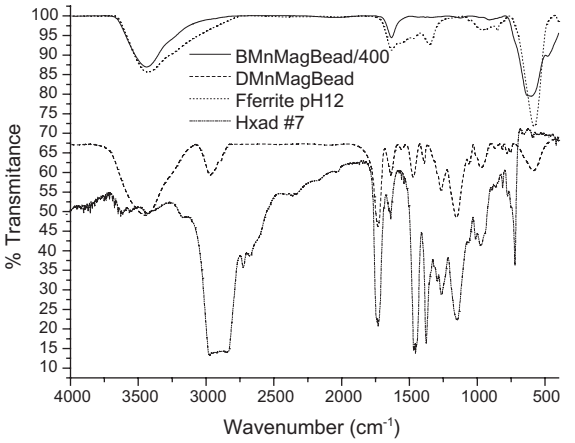

Fig. 2. FTIR spectra of Amberlite XAD#7, $MnFe_2O_4$, MnMagBead particles, and MnMagBead particles thermically treated at 400 °C.

to the water molecules in the MnMagBeads. In the range of 159.82–517.58 °C resin degradation occurs with a mass loss of 35.1% and a third event was observed in the interval of 517.58–990.78 °C (27.1%) and was attributed to decomposition of other phases formed in the precipitation differing from $MnFe_2O_4$. On the other hand, it is verified that at 990.78 °C the residual solid (29.3%) was produced and above this temperature, there is no mass loss [30].

MnMagBeads exhibited a strong magnetization in the presence of a magnetic field, displaying an excellent magnetic response, as shown in Fig. 4.

In order to study their magnetic behavior, magnetization measurements were performed. Fig. 5(A) shows, the magnetization curve, registered for MnMagBeads resin and it could be observed that there is no hysteresis and a complete reversibility at 300 K was found: it is more clearly denoted in the insert (B) of Fig. 5, where neither coercivity nor magnetic remanence in MnMagBeads resin is observed corroborating with a typical superparamagnetic behavior [31], a feature that is not in accordance with what should be expected from their particle size (XAD#7 0.3–1.2 mm). Superparamagnetism is exhibited by magnetic particles with a size below a critical diameter [31]. An approximated value of superparamagnetic critical size, Dp; for spherical manganese ferrite particles

Table 1
Attributions of infrared spectra of the materials

Materials	Transitions (cm^{-1})
Acrylate XAD#7	ν_{O-H} 3439, νass_{CH_2} 2966, $\nu_{C=O}$ 1733, δ_{O-H} 1640, δ_{CH} 1148, δ_{O-H} 973
$MnFe_2O_4$	ν_{O-H} 3439, δ_{O-H} 1637, $\nu_{M_{Td}-O-M_{Oh}}$ 579 cm^{-1}
$MnFe_2O_4$-400	ν_{O-H} 3439, δ_{O-H} 1637, $\nu_{M_{Td}-O-M_{Oh}}$ 638–589 cm^{-1}, 400 cm^{-1}
MnMagBead	ν_{O-H} 3439, νass_{CH_2} 2966, $\nu_{C=O}$ 1731, δ_{O-H} 1637, δ_{CH_3} 1477, 1394, δ_{CH} 1157, δ_{O-H} 966, and $\nu_{M_{Td}-O-M_{Oh}}$ 580 cm^{-1}

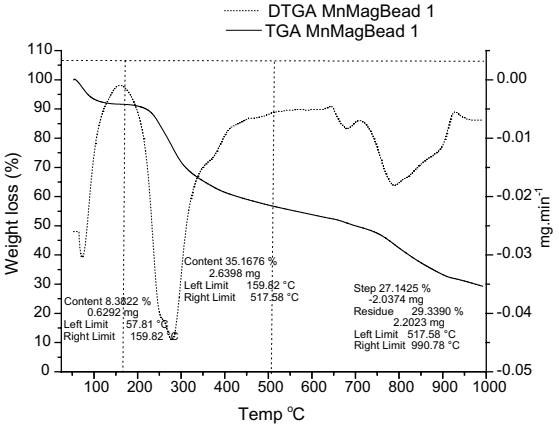

Fig. 3. TGA/DTGA curves for MnMagBead particles.

Fig. 4. MnMagBead particles being attracted by a magnet.

was calculated in our case from expression (1), due to the time of measurement of magnetic field be equal to 1 s:

$$V_s \approx \frac{21kT}{K}, \tag{1}$$

where k is the Boltzmann constant, K is the anisotropy constant ($MnFe_2O_4 = 0.3 \times 10^5$ ergs cm^{-3} [31] and T is the absolute temperature. For this case where T is 300 K, the estimated Dp is equal to 38.10 Å. Another important parameter for the practical application of MnMagBeads is their magnetization. Due to the asymptotic increase of magnetization for high fields (see the insert (C) of Fig. 5), the saturation magnetization value can be obtained through the fitting of the M versus $1/H$ curve, extrapolating the magnetization value to $1/H = 0$ [32]. The saturation magnetization found for MnMagBead particles is 55.73 emu g^{-1}, which is lower than that of bulk $MnFe_2O_4$ 80 emu g^{-1} [31]. This decrease in saturation magnetization can be attributed to attenuated surface effects such as magnetically inactive layers containing spins that are not collinear with the magnetic field and the small size of ferrite particles [33–36]. We observed a discrepancy in the magnetization saturation values reported in the literature, and this could be explained through the methods used in the synthesis process that generate particles with different sizes, surfaces and chemical compositions [37]. The magnetization saturation value obtained herein corroborate with the range of values reported in the literature [38,39]. From the slope of the magnetization curve near $H = 0$, the diameter of the superparamagnetic MnMagBeads can be estimated [40] according to the expression (2),

$$D_{mag} = \left(\frac{18kT(dM/dH)_0}{\pi\rho M_s^2}\right)^{1/3}, \tag{2}$$

where k is the Boltzmann constant, T is the absolute temperature, $(dM/dH)_0$ is the initial slope of the magnetization curve near the origin, ρ is the density of $MnFe_2O_4$ 5.0 g cm^{-1} [31], and M_s is the saturation magnetization. Taking the saturation magnetization obtained for manganese ferrite

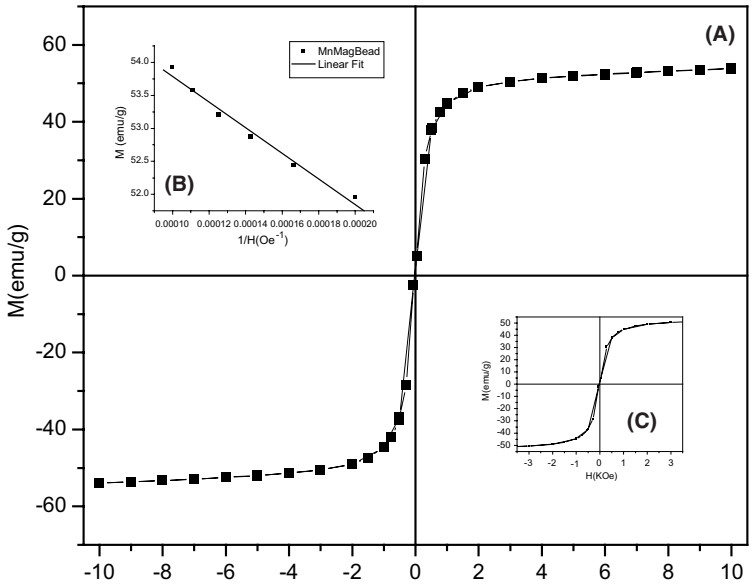

Fig. 5. Magnetization curve of MnMagBeads at 300 K.

55.73 emu g^{-1}, a diameter equal to 36.6 Å nm was found, which is smaller than that for XAD#7 channel diameter (39%) and approximately equal to that calculated by Eq. (1) (4%). This difference could result from the extrapolated saturation magnetization value and from particle surface effects such as magnetically inert templates, the density of the manganese ferrite, used for calculation, which does not necessarily correspond to that of the true phase composition, contributing to this little discrepancy.

Table 2 shows the behavior of absorption of BSA in the MnMagBead particles. The result shows the profile of these beads as a function of the contact time. We observed a maximum retention in 60 min of contact followed by a decrease in the absorption after 180 min showing the reversion of the process. The maximum retention of BSA by this material achieved in the buffer medium studied (5×10^{-6}) μg of BSA/100 mg of dried beads. The capacity of this material is not high, but is better than that of chitosan/$MnFe_2O_4$ beads also studied in our laboratory, which presented no adsorption. Some adjustments using efficient linkers and functionalizing the polymer chain is expected to improve this absorption and is now being done in our laboratory.

Table 2
Behavior of ^{125}I-BSA adsorption with time

Time (min)	Adsorption (μg/100 mg of dry beads)
30	2.73
60	3.3

4. Conclusions

This method describes the preparation of magnetic particles by controlling their size using a polymeric template. The MnMagBeads were characterized by FTIR, TGA/DTGA and magnetic measurements. The IR results agree with no interaction between the magnetic core and the polymer template. The TGA/DTGA showed three events in the thermal decomposition until we obtained the thermically treated ferrite. The magnetic measurements showed that particles have a size smaller than the diameter of bead channels and close to the critical size to exhibit superparamagnetic behavior.

MnMagBead particles are superparamagnetic and they respond to magnetic fields but do not

retain magnetic properties upon removal of the magnetic field. This inability to become magnetized permits magnetic extraction without magnetically induced aggregation. Rapid and efficient removal of MnMagBead particles from the suspension is achieved by application of an external magnetic field facilitating the experimental procedure.

These superparamagnetic beads exhibit the capability to bind biological molecules such as proteins like BSA with a good capacity (5×10^{-6}) μg/100 mg of beads when compared with chitosan/$MnFe_2O_4$ beads (with no adsorption).

Acknowledgments

The authors are grateful to Dr. M.T.C.P. Ribela and to the Fundação de Amparo à Pesquisa do Estado de São Paulo (FAPESP) and the Conselho Nacional de Desenvolvimento Científico e Tecnológico (CNPq-RENAMI) for financial support.

References

[1] K. Rajeshwar, N.R. de Tacconi, C.R. Chenlhamarakshan, Chem. Mater. 13 (2001) 2765.
[2] L. Zhang, G.C. Papaefthymiou, J.Y. Ying, J. Phys. Chem. B 105 (2001) 7414.
[3] P.C. Moraes, R.B. Azevedo, D. Rabelo, C.D. Lima, Chem. Mater. 15 (13) (2003) 2485.
[4] P. Kronick, R.W. Gilpin, J. Biochem. Biophys. Methods 12 (1986) 73.
[5] X. Liu, H. Liu, J. Xing, Y. Guan, Z. Ma, G. Shan, C. Yan, Ch. Particuol. 1 (2) (2003) 76.
[6] X.H. Li, Z.H. Sun, J. Appl. Polym. Sci. 58 (1995) 1991.
[7] T. Abudian, R.R. Beitle, J. Chromatogr. A 795 (1998) 211.
[8] P.A. Cuspa, C.T. Hung, Life Sci. 44 (1989) 175.
[9] Z.L. Liu, Z.H. Ding, K.L. Yoo, J. Tao, G.H. Du, Q.H. Lu, X. Wang, F.L. Gong, X. Chen, J. Magn. Magn. Mater. 265 (2003) 98.
[10] X.B. Ding, Z.H. Sun, G.X. Wan, Y.Y. Jiang, React. Funct. Polym. 38 (1998) 11.
[11] P.J. Robinson, P. Dunnil, M.D. Lilly, Biotechnol. Bioeng. 15 (1973) 603.
[12] J. Ugelstad, A. Berge, T. Ellingsen, R. Schmid, T.N. Nilsen, P.C. Mork, P. Stenstad, E. Horenes, O. Olsvik, Prog. Polym. Sci. 17 (1992) 87.
[13] T.O. Ely, C. Amiens, B. Chaudret, Chem. Mater. 11 (1999) 526.
[14] M.R. Ayes, X.Y. Song, A.J. Hunt, J. Mater. Sci. 31 (1996) 6251.
[15] L. Chen, W.J. Yang, C.Z. Yang, J. Mater. Sci. 32 (1997) 3571.
[16] S. Ramesh, R. Prozorov, A. Gedanken, Chem. Mater. 9 (1997) 2996.
[17] E. Kroll, F.M. Winnik, R.F. Ziolo, Chem. Mater. 8 (1996) 1594.
[18] D. Horak, J. Polym. Sci., A, Polym. Chem. 39 (2001) 3707.
[19] D. Horak, J. Bohacek, M. Subrt, J. Polym. Sci., A, Polym. Chem. 38 (2000) 1161.
[20] V.S. Gurin, V.B. Prokopenko, I.M. Melnichenko, E.N. Poddenezhny, A.A. Alexeenko, K.V. Yumashev, J. Non-Cryst. Solids 232–234 (1998) 162.
[21] Y.P. Sun, H.W. Rollins, R. Guduru, Chem. Mater. 11 (1999) 7.
[22] A. Wooding, M. Kilner, D.B. Lambrick, J. Colloid Interf. Sci. 144 (1991) 236.
[23] Y.S. Kang, S. Risbud, J.F. Rabolt, P. Stroeve, Chem. Mater. 8 (1996) 2209.
[24] M. Yamaura, R.L. Camilo, M.C.F.C. Felinto, J. Alloy Compd. 344 (2002) 152.
[25] M. Yamaura, R.L. Camilo, L.C. Sampaio, M.A. Macêdo, M. Nakamura, H.E. Toma, J. Magn. Magn. Mater. 279 (2004) 210.
[26] A.A.A. Queiroz, S.C. Castro, O.Z. Higa, J. Biomater. Sci. Polymer. Edn. 8 (1997) 335.
[27] http://www.sigmaaldrich.com/Brands/Supelco_Home/Datanodes.html?cat_path = 989104&id = 989104 & supelco_name = Air%20Monitoring 09/22th/2004.
[28] R.W. Waldron, Phys. Rev. 99 (1955) 1727.
[29] N. Shukla, C. Liu, P.M. Jones, D. Weller, J. Magn. Magn. Mater. 266 (2003) 178.
[30] P.J. Haines, Thermal Methods as Analysis. Principles, Applications and Problems, first ed., Chapman & Hall, London, 1995.
[31] B.D. Cullity, Introduction to Magnetic Materials, Addison Wesley Publishing Company, 1972.
[32] C. Liu, Z.J. Zhang, Chem. Mater. 13 (2001) 2092.
[33] D.H. Han, J.P. Wang, Y.B. Feng, H.L. Luo, J. Appl. Phys. 76 (1994) 6591.
[34] D. Lin, A.C. Nunes, C.F. Majkrzak, A.E. Berkowitz, J. Magn. Magn. Mater. 145 (1995) 343.
[35] T. Sato, T. Iijima, M. Seki, N. Inagaki, J. Magn. Magn. Mater. 65 (1987) 252.
[36] R.H. Kodama, J. Magn. Magn. Mater. 200 (1999) 359.
[37] M. Grigorova, H.J. Blythe, V. Blaskov, V. Rusanov, V. Petkov, V. Masheva, D. Nihtianova, L.M. Martinez, J.S. Munõz, M. Mikhov, J. Magn. Magn. Mater. 183 (1998) 163.
[38] R.D. Ambashta, P.K. Wattal, S. Singh, D. Bahadur, J. Magn. Magn. Mater. 267 (2003) 335.
[39] P.A. Heiney, K. Gruneberg, J. Fang, C. Dulcey, R. Shashidhar, Langmuir 16 (2000) 2651.
[40] N.A.D. Burke, H.D.H. Stover, F.P. Dawson, Chem. Mater. 14 (2002) 4752.